

MICROCOPY RESOLUTION TEST CHART
NATIONAL BUREAU OF STANDARDS-1963-A

12

AD-A161 688

Final Report for

Grant No. N00014-83-K-0263

MODIFICATIONS IN MICROSTRUCTURE, DEFORMATION
AND FATIGUE BEHAVIOR BY ION IMPLANTATION

Submitted to:

Office of Naval Research
800 N. Quincy Street
Arlington, VA 22217-5000

Attention: Leader, Materials Division
Associate Director for
Engineering Sciences

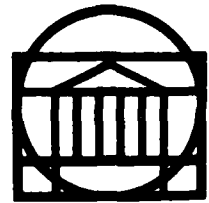
Submitted by:

K. V. Jata
Research Assistant Professor
E. A. Starke, Jr.
Earnest Oglesby Professor and Dean

SDTIC
ELECTE
NOV 27 1985
S E D

Report No. UVA/525386/MS86/101

October 1985



SCHOOL OF ENGINEERING AND
APPLIED SCIENCE

DEPARTMENT OF MATERIALS SCIENCE

UNIVERSITY OF VIRGINIA

CHARLOTTESVILLE, VIRGINIA 22901

This document has been approved
for public release and sale; its
distribution is unlimited.

85 11 25 096

FILE COPY

Final Report on

Grant No. N00014-83-K-0263

MODIFICATIONS IN MICROSTRUCTURE, DEFORMATION
AND FATIGUE BEHAVIOR BY ION IMPLANTATION

Submitted to:

Office of Naval Research
800 N. Quincy Street
Arlington, VA 22217-5000

Attention: Leader, Materials Division
Associate Director
for Engineering Sciences

Submitted by:

K. V. Jata
Research Assistant Professor
E. A. Starke, Jr.
Earnest Oglesby Professor and Dean

Department of Materials Science
SCHOOL OF ENGINEERING AND APPLIED SCIENCE
UNIVERSITY OF VIRGINIA
CHARLOTTESVILLE, VIRGINIA

Report No. UVA/525386/MS86/101
October 1985

Copy No. _____

This document has been approved
for public release and sale; its
distribution is unlimited.

SECURITY CLASSIFICATION OF THIS PAGE (When Data Entered)

REPORT DOCUMENTATION PAGE		READ INSTRUCTIONS BEFORE COMPLETING FORM	
1. REPORT NUMBER	2. GOVT ACCESSION NO.	3. RECIPIENT'S CATALOG NUMBER	
	AD-A161 688		
4. TITLE (and Subtitle) Modifications in Microstructure, Deformation and Fatigue Behavior by Ion Implantation		5. TYPE OF REPORT & PERIOD COVERED Final Report 3/1/83 - 5/31/85	
		6. PERFORMING ORG. REPORT NUMBER UVA/525386/MS86/101	
7. AUTHOR(s) K. V. Jata and E. A. Starke, Jr.		8. CONTRACT OR GRANT NUMBER(s) N00014-83-K-0263	
9. PERFORMING ORGANIZATION NAME AND ADDRESS Department of Materials Science University of Virginia Charlottesville, VA 22901		10. PROGRAM ELEMENT, PROJECT, TASK AREA & WORK UNIT NUMBERS	
11. CONTROLLING OFFICE NAME AND ADDRESS Leader, Materials Division Office of Naval Research 800 N. Quincy St., Arlington, VA 22217		12. REPORT DATE	
		13. NUMBER OF PAGES 15	
14. MONITORING AGENCY NAME & ADDRESS (if different from Controlling Office)		15. SECURITY CLASS. (of this report) Unclassified	
		15a. DECLASSIFICATION/DOWNGRADING SCHEDULE	
16. DISTRIBUTION STATEMENT (of this Report) Unlimited			
<div style="border: 1px solid black; padding: 5px; display: inline-block;"> This document has been approved for public release and sale; its distribution is unlimited. </div>			
17. DISTRIBUTION STATEMENT (of the abstract entered in Block 20, if different from Report)			
18. SUPPLEMENTARY NOTES			
19. KEY WORDS (Continue on reverse side if necessary and identify by block number) ion plating, ion implantation, fatigue			
20. ABSTRACT (Continue on reverse side if necessary and identify by block number) A number of materials, copper, aluminum, titanium and steel, have been examined for microstructural evolution, deformation and fatigue behavior in the non-implanted, as-implanted and implanted + annealed conditions. A wide variety of implant species that produce residual compressive stresses, residual tensile stresses or cause precipitation have been chosen to examine the above effects. The main goal has, however, been to choose implant species that would enhance deformation and fatigue resistance through a modification in the surface microstructure and/or by providing residual compressive stresses. (CONTINUED)			

In instances where no major changes in the surface microstructure are observed it appears that surface dislocation sources either become inoperative or become operative on a larger number of slip planes, limiting the size of the slip steps that would nucleate fracture. In materials where major changes in the microstructure are observed, slip is dispersed, also resulting in fine slip that enhances resistance.

Accession For	
NTIS GRA&I	<input checked="" type="checkbox"/>
DTIC TAB	<input type="checkbox"/>
Unannounced	<input type="checkbox"/>
Justification	
By	
Distribution/	
Availability Codes	
Dist	Avail and/or Special
A-1	



1. Introduction

This paper will review work on surface modification of materials by ion plating and ion implantation that was sponsored by the Office of Naval Research under the Program Direction of Dr. Phillip Clarkin. Ion implantation is being used to modify surface-related mechanical properties such as friction and wear, fatigue, corrosion and recently, near surface deformation at high temperatures, (1-5). The major thrust has been in friction and wear, since small doses of implanted atoms produce large effects. Application to fatigue mainly stems from the fact that the fatigue cracks normally nucleate at the surface of a structure and propagate inward. The fatigue process may be divided into two stages, which are crack initiation and crack propagation. For a defect-free metal, the process of initiation and early micro crack linkage is usually associated with the cyclic deformation behavior of the surface layer. This process is found to occur in conjunction with slip band formation (6) in the surface region, or with incompatibility of deformation between two neighboring grains on the surface (7,8). Any surface modification which reduces the magnitude or increases the homogeneity and reversibility of cyclic deformation is expected to improve the fatigue crack initiation resistance. Surface modification of materials can be achieved by a number of techniques such as shot peening, nitriding, ion plating, ion implantation and laser glazing. Of these, ion implantation has several unique advantages that the other techniques do not offer. It has the advantage of introducing almost any ion substitutionally and interstitially into the target substrate without affecting the desirable bulk properties. There are no dimensional changes and problems such as delamination of the layer do not exist. The dose of ions could be introduced in a well controlled manner and the property changes can therefore be easily reproduced. Although the implanted layer is usually a few hundred to a thousand angstroms thick substantial changes in fatigue properties can be observed. This paper will give an overview of the various effects that ion implantation can have on microstructure, deformation behavior and fatigue crack initiation resistance. The materials include pure Cu, pure Al, two titanium alloys, 4140 steel and a 2124 Al alloy.

2. Discussion of Results

In this section the results of ion implantation effects on various materials are discussed. We start with pure copper as this formed the basis of further work on complex alloys. Next, microstructural evolution in pure Al is discussed. This is followed by the discussion of ion implantation effects in commercial alloys.

2. A. Ion Plating and Implantation Effects in Cu

The initial work carried out by Chen and Starke (9) have shown that ion plating can have a major effect on the fatigue behavior of copper single and poly crystals. When they plated silver (low Stacking fault energy, SFE) on copper, the cyclic deformation behavior of the surface changed toward that of silver. Crack initiation was retarded because of a reduction in the propensity of cross slip compared with the copper substrate and subsequent reduction of slip band formation. Nickel (high SFE) plating had an opposite effect.

Ion implantation studies were later performed on polycrystalline copper (4,10) to obtain a clear understanding of the mechanisms involved in the modification of fatigue properties. The purpose of the work was to study the change in monotonic and cyclic deformation behavior of copper with three different species - aluminum, boron and chromium - and to correlate measured mechanical properties with the deformation behavior of as modified by ion implantation. It was expected that all three elements will introduce a similar defect structure but of varying degrees of intensity. Also, boron atoms, because of their small size with respect to copper, were expected to introduce tensile residual surface stresses, and aluminum atoms because of their larger size were expected to introduce compressive stresses. X-ray diffraction results (11) of aluminum and boron implanted copper single crystals have shown this to be the case.

Specimens were implanted at 100 keV with either aluminum, boron or chromium ions to a dose of 5×10^{19} ions/m². To insure uniformity of implantation, the specimens were rotated in the beam which was scanned across an aperture spanning the gage length. Fatigue tests of ion implanted and non-implanted samples were conducted on a servohydraulic closed-loop testing machine in laboratory air at 298 K. Low cycle fatigue measurements were made using constant total strain control with a saw-tooth wave form at a strain rate of 4×10^{-3} /s. Stress control, high cycle fatigue tests were made using a frequency of 10 Hz.

The monotonic stress-strain curves of the various materials are given in Figure 1(a). The figure shows that ion implantation reduces the flow stress at low strains. The reduction in stress is largest for the aluminum-implanted sample. The monotonic yield stress and degree of hardening appear to be reduced due to ion implantation, with aluminum implantation having a somewhat larger effect. The cyclic stress-strain response studies showed all materials to considerably cyclic harden typical of annealed copper. An initial rapid hardening is followed by a saturation stage. The saturation stress versus applied plastic strain amplitude for nonimplanted and implanted metals are plotted in Figure 1(b). The cyclic flow stress appears to be lowered by ion implantation. Alumi-

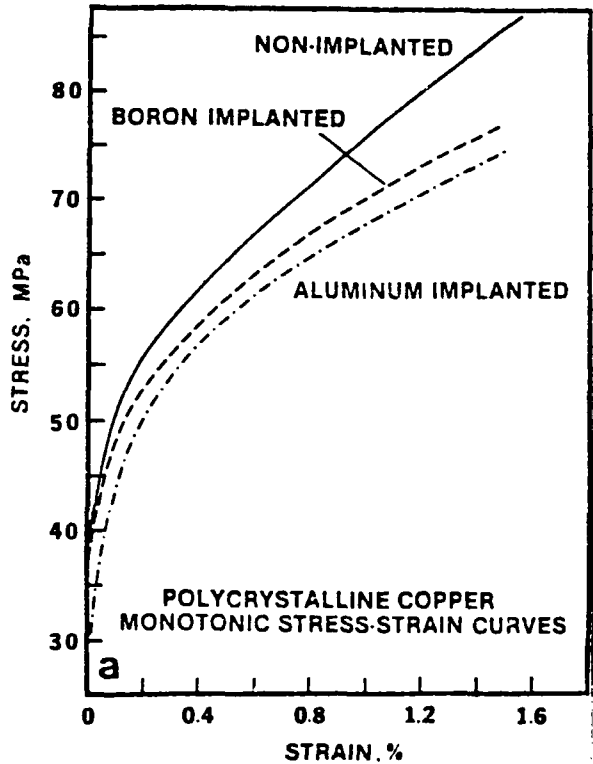


Fig. 1(a). The effect of ion implantation on monotonic stress-strain curve of polycrystalline copper.

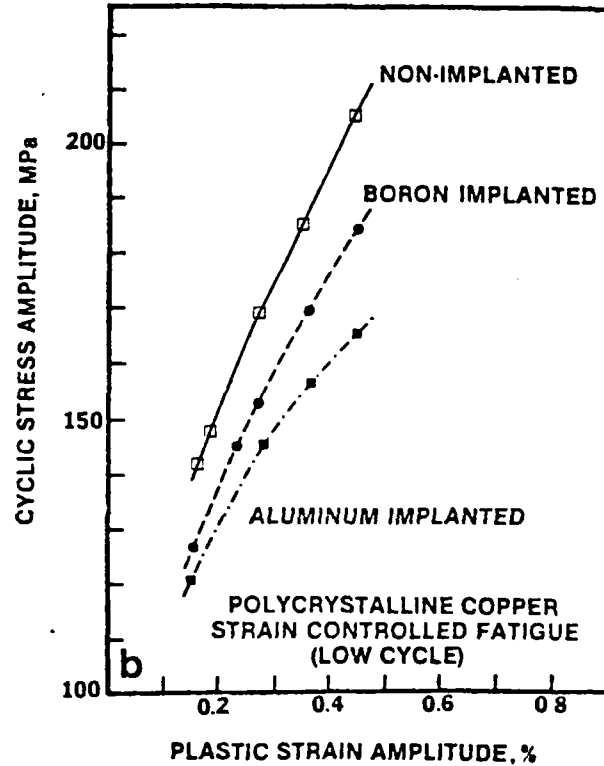


Fig. 1(b). The effect of ion implantation on cyclic stress-strain relationship of polycrystalline copper.

num implantation again shows the most significant effect. The cyclic strain-life response (LCF) for the nonimplanted and implanted polycrystalline copper are presented in Figure 2(a). The relationship between the number of cycles to failure and the plastic strain amplitude may be represented by a power function proposed by Coffin and Manson, given by $\epsilon_{pa} = \epsilon_f (2N_f)^c$, where N_f is the number of cycles to failure, ϵ_f is the fatigue ductility coefficient and c is the fatigue ductility exponent. This relationship appears to hold for the materials tested in this research. The results indicate that ion implantation improves the fatigue ductility behavior. Aluminum implantation appears to have the most significant effect.

The effect of ion implantation on the high cycle fatigue life is shown in Figure 2(b). Aluminum implantation gives rise to a significant improvement in fatigue life, with a greater improvement at lower stresses. Boron implantation, in contrast, shows a reduction in resistance to cyclic stress, with a greater reduction in life at lower stresses. The limited data on chromium implantation appeared to indicate that it improves the cyclic stress resistance almost as well as aluminum implantation.

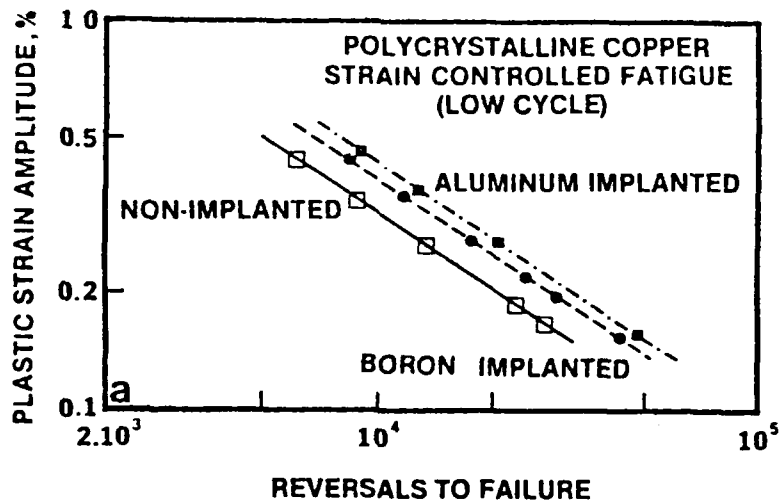


Fig. 2a. The effect of ion implantation on cyclic strain-life relationship of polycrystalline copper.

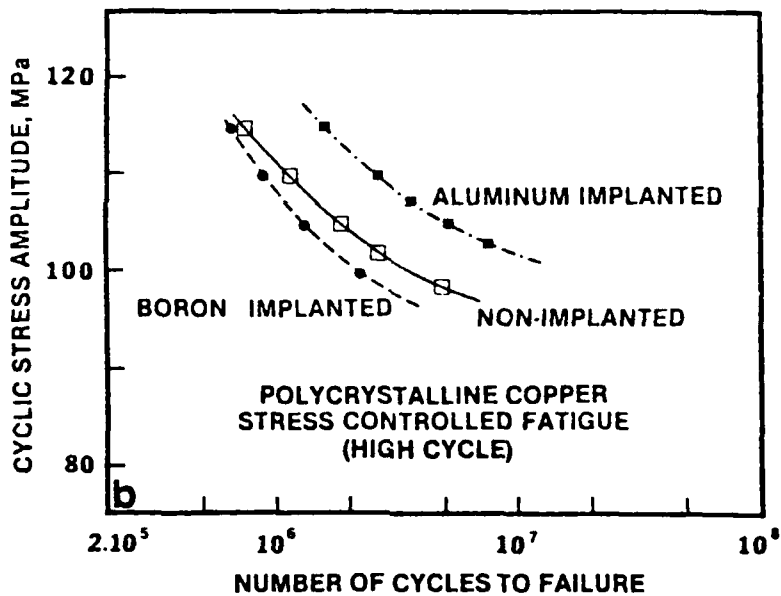


Fig. 2(b). The effect of ion implantation on cyclic stress-life relationship of polycrystalline copper.

The surface observations of the strain controlled fatigued samples showed the presence of persistent slip bands (PSB) and associated intrusions/extrusion. However, the propensity of PSB formation appeared to be reduced by ion implantation. Aluminum implantation had the most significant effect. Most of the microcracks were at the grain boundaries. Some cracks associated with PSB were also observed, being more frequent for the non-implanted samples and least for the aluminum implanted samples. Implanted samples showed a lower degree of surface rumpling and fewer surface microcracks compared with nonimplanted samples deformed to the same degree. The stress controlled fatigue samples showed cracking to be more prominent with PSB than that of strain controlled fatigue samples.

The TEM results and the X-ray analysis by Spooner and co-workers (11) indicated that aluminum implantation gives rise to compressive residual surface stresses, a large number of small dislocation loops, and arrays of dislocations. Boron implantation, on

the other hand, produces tensile residual stresses, a smaller number of larger loops, and dislocation arrays. Since the size of the chromium atom is not much different from that of copper, it may be assumed that chromium implantation does not produce any significant residual surface stresses. If the increase in the numbers of atoms by ion implantation forces implant or host atoms into the interstitial sites, creation of compressive residual stresses will be expected. However, with some diffusion (probably enhanced by radiation damage) these form an extra atom layer occupying substitutional sites (such a mechanism is reasonable since TEM studies showed that there is sufficient diffusion to create dislocation loops from the initial radiation damage). Therefore, significant compressive stress will not be created due to interstitials. This may explain why boron implanted copper has tensile residual stresses. Perhaps most of the boron atoms are in substitutional sites, and since they are considerably smaller than the copper atoms, tensile residual stresses are created. TEM contrast studies of some of the loops indicated that most are the result of a collapse of clusters of vacancies created by ion bombardment. It appears that since heavier (and larger) Cr and Al atoms have a more efficient transfer of energy than B atoms, the defect structure of Cr and Al implanted surfaces has greater density. Since the foils used for TEM observations are thicker than the damaged layer (which decreases with atomic number), the concentration of defects is actually even higher for Cr and Al implanted samples than it appears in their micrographs. In addition to the defect structure and residual surface stresses, the alloying of the surface material is expected to lower the stacking fault energy (SFE) of this region. It is likely that precipitation of chromium will occur in the chromium implanted samples during fatigue cycling. The effect of lowering SFE will be lost at that stage, and the presence of chromium precipitates has to be considered instead.

The implantation of Al, B, or Cr ions lowers the yield stress and the degree of monotonic and cyclic hardening. The reduction in yield stress and monotonic hardening at low strains is perhaps due to the availability of free dislocations on the surface which tends to promote slip at lower stresses. Aluminum implantation, which produces a larger degree of surface defects, consequently shows a larger reduction of monotonic flow stress.

The reduction of cyclic hardening was explained in terms of the lowering of the SFE and the presence of dislocation loops and arrays due to ion-implantation. Lowering the SFE leads to a reduction in the tendency for cross slip. This improves the reversibility of cyclic deformation and reduces cyclic hardening. Dislocation loops are barriers to slip and tend to homogenize deformation by reducing the slip distance. Improved homogeneity of slip due to implantation aids in reducing the resistance to cyclic deformation. Aluminum implanted samples have a higher degree of surface defects, the greatest reduction in hardening, and therefore the lower cyclic flow stresses. The chromium implanted samples have a similar defect structure. However, it appears that Cr precipitation during cycling increases cyclic hardening somewhat by tying up slip dislocations.

Under strain controlled fatigue the microcrack formation and eventual failure of the materials follow what is expected from the foregoing discussion of the cyclic hardening behavior. The effect of ion implantation is to improve slip reversibility and homogeneity, and in general this leads to improvement in the low cycle fatigue life, regardless of the exact mechanism of cracking. The difference between the FCI resistance of boron and aluminum implanted samples is again due to the difference in defect structure. Aluminum implantation produces the most significant effect because it gives rise to a more intense defect structure. Even though chromium implantation results in a defect structure similar to aluminum, the expected intervention of chromium precipitation decreases the resistance to FCI under what is expected from its defect structure.

Under stress control the ion implanted samples are expected to show improvement in fatigue life due to better slip homogeneity and reversibility. However, other parameters must be considered. Aluminum implanted samples have beneficial compressive surface stress. The compressive stress tends to reduce the more damaging (i.e., tensile) component of the cyclic stress and hence improves the fatigue life. The tensile residual surface stress produced by boron implantation decreases the resistance to stress cycling. The beneficial effects of surface defects due to implantation are overcompensated by the detrimental effects of the residual tensile surface stresses.

2. B. Microstructural Studies of Pure Aluminum

Ion implantation offers the possibility of obtaining alloys having: (i) a highly supersaturated solid solution with extended solid solubility over that predicted by the phase diagram; (ii) a solid solution with stable and metastable phases; and (iii) a disordered or amorphous structure in metal-metal or metal-metalloid systems. In many instances, alloy systems produced by rapid quenching have been duplicated by ion implantation (12,13) and parallels have been drawn between the two techniques. In ion implantation the thermal spike concept (14) suggests that local heating of the target could take place on the impingement of an ion with energy values of the order of 50-500keV. The temperatures in the hot zone produced by the thermal spike could exceed the melting point of the solid, however the time scale of the thermal spike is only a few pico-seconds resulting in an ultra fast quench of the molten zone. Consequently the diffusion required to form the metastable and stable phases cannot occur during the thermal spike. A second theory suggests that some precipitation could however, occur due to radiation enhanced diffusion (15) which depends on the defect production rate and number of dislocations per unit area, since the radiation enhanced diffusion coefficient is many orders of magnitude larger than the thermal diffusion coefficient. The former phenomenon where a supersaturated solid solution exceeding the solubility limits of the solute can be obtained at room temperature is similar to the rapid solidification technique. The above concepts have been used in aluminum implanted with Fe (16). Iron has a solubility limit of 0.05 wt. percent and a diffusivity of only $4.1 \times 10^{-13} \text{ m}^2/\text{sec}$ and in normal wrought alloys is present as large inclusions which are detrimental to fatigue life. So, by adopting ion implantation technique it should be possible to obtain a fine dispersion of Al_6Fe or Al_3Fe precipitates which would homogenize slip and thereby improve fatigue life.

Discs of high purity Al of Marz grade quality with $3 \times 10^{-3} \text{ m}$ diameter and $2.54 \times 10^{-4} \text{ m}$ thickness were prepared. These discs were then thinned in a methanol-nitric acid electrolyte and subsequently implanted with iron on one face. Two energies were used, 50 and 100+50keV and the doses were 5×10^{19} and 5×10^{20} ions/ m^2 . The double dosage 100+50keV, implantation was performed with a time interval of one hour between the 100 and 50 keV implantations. The temperature rise of the discs during implantation is estimated to be less than 373k. Electrothinning was then completed by masking the implanted face with a lacquer. The thin foils were subsequently examined in TEM.

For both 50 and 100 + 50 keV dosages, extensively damaged substructure typical of ion implanted materials was observed. In Figure 3(a) a bright field transmission electron

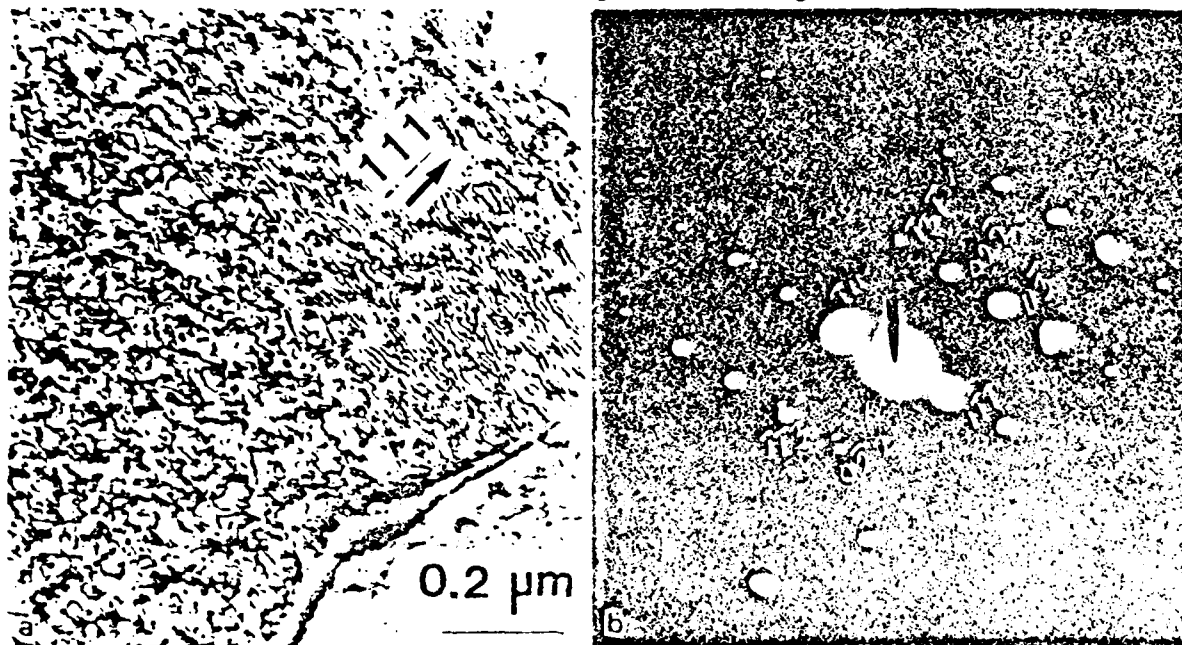


Fig. 3. TEM's of 50 keV as-implanted showing modulations in $\langle 111 \rangle$ direction and damage (a), SAD of modulations showing satellites (b).

micrograph for a 50 keV Al implanted foil is shown. The left part of the micrograph shows the implantation damage and the right part shows a typical modulated structure observed in these foils. The composition fluctuations in the modulation are found to be in $\langle 111 \rangle$ direction and 10 nm apart. The corresponding electron diffraction pattern, Figure 3(b) of the modulated structure shows satellite spots near the Bragg reflections. These satellite spots are not observed due to the presence of dislocation defects produced by implantation. It was difficult to observe the modulated structure under two beam conditions since this structure was masked by the implantation damage which comes under view for maximum contrast conditions. Moire fringes were also observed in the areas of the modulated structure. As expected, these fringes shifted their relative position with respect to the modulated structure as the specimen was tilted in the stage around the axis of the transmitted electron beam path. Thus, it was clearly possible to distinguish between the modulated structure and the Moire fringes. The micrograph Fig-

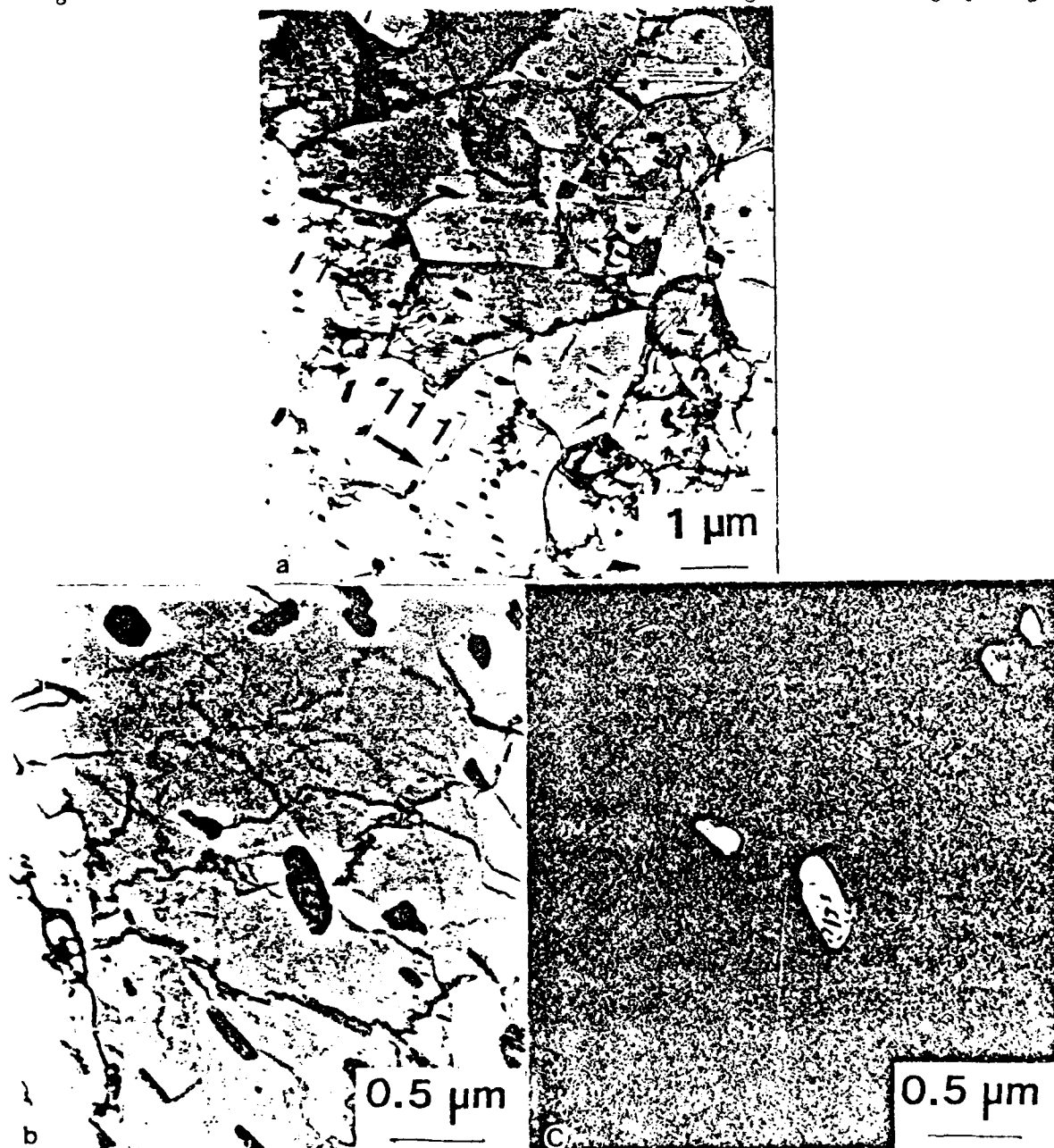


Fig. 4. TEM's of 50 keV + 30 min. annealing at 793 K showing Al_3Fe precipitates aligned along $\langle 111 \rangle$ direction (a), bright and dark field of images of Al_3Fe (b) and (c).

ure 4(a) was taken using the conditions when the fringes and the damaged structure were completely out of view. A further confirmation of the presence of the modulated structure was obtained from the 100 + 50 keV foil which was given an annealing treatment at 793 K for 15 minutes. This treatment removed the extensive damage resulting from the double dosage ion implantation. The micrographs clearly revealed rod-like precipitates and many areas of retained modulated structure. The 50 keV foils were also examined after an annealing treatment of 30 minutes at 793K. Al₃Fe precipitates were observed which were aligned in the <111> direction with respect to the matrix. These precipitates are shown in Figure 4(a). A higher magnification pair of bright and dark field micrographs are shown in Figure 4(b) and (c). The growth of these precipitates seems to bear an orientation relationship with the composition fluctuations found along <111> direction in Figure 3(a). Figure 4(a) might also imply that the modulations in regions where the subgrain boundaries are tilted at small angles prefer the same orientation.

2. C. Fatigue Studies of Commercial Alloys

The concepts developed for pure copper were latter applied to commercial alloys. A binary Ti-24V (17) alloy implanted with Al ions at 100 keV to a dose of $5 \times 10^{19} / \text{m}^2$ showed a minor improvement in the fatigue life at intermediate plastic strain amplitudes (Figure 5). An examination of the fatigue hysteresis loops for these amplitudes showed that the number of cycles to reach saturation stress increased by about 40 percent with Al implantation. In order to understand the beneficial effect of ion implantation on the fatigue behavior additional experiments were run, where biode replicas were extracted from the specimen surface at different intervals of cycles during the course of the fatigue experiment. The biode replicas were carbon shadowed at an angle of 30 degrees to the stress axis and were observed under an optical microscope. A pair of micrographs illustrating the difference in the slip activity on the surface at a plastic strain amplitude of 8×10^{-3} and at 150 cycles is shown in Figure 6. It is clear that the non-implanted specimen exhibits a number of parallel slip lines, suggesting major activity in only one slip system. With continued cycling, slip is concentrated along these lines, eventually leading to slip band cracking. In Figure 6(b) it can be clearly seen that Al implantation homogenizes slip. The slip is accommodated in more than one slip system and thus the slip lines remain fine with continued cycling. Cracks were initiated only at grain boundaries where the slip lines impinge. No cracks were observed at slip line intersections. It is however surprising, that in spite of a major change in the mode of cyclic slip behavior the fatigue life changed so little.

In stress controlled experiments the beneficial effect of ion implantation is observed at all stress levels employed for testing, Figure 7. In these tests the tensile component of the stress amplitude ranged between 0.6 and 0.85 of the monotonic yield stress. At

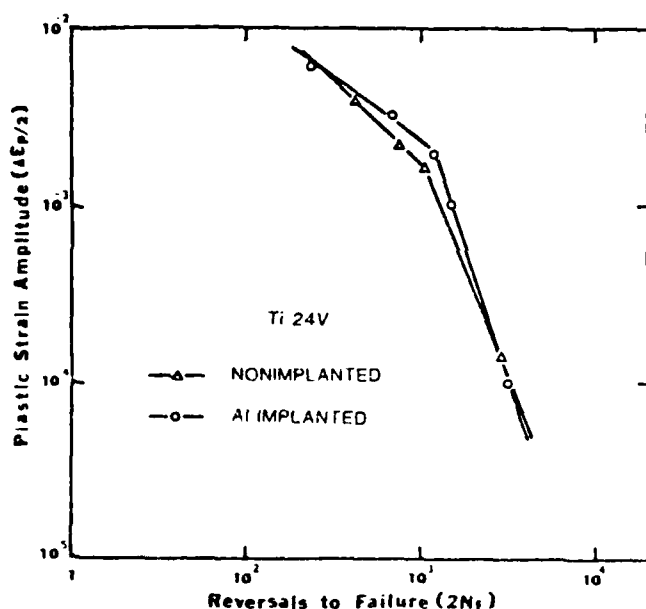


Fig. 5. Coffin-Manson plot showing the plastic strain amplitude versus number of cycles to failure for the Ti-24V Al alloy.

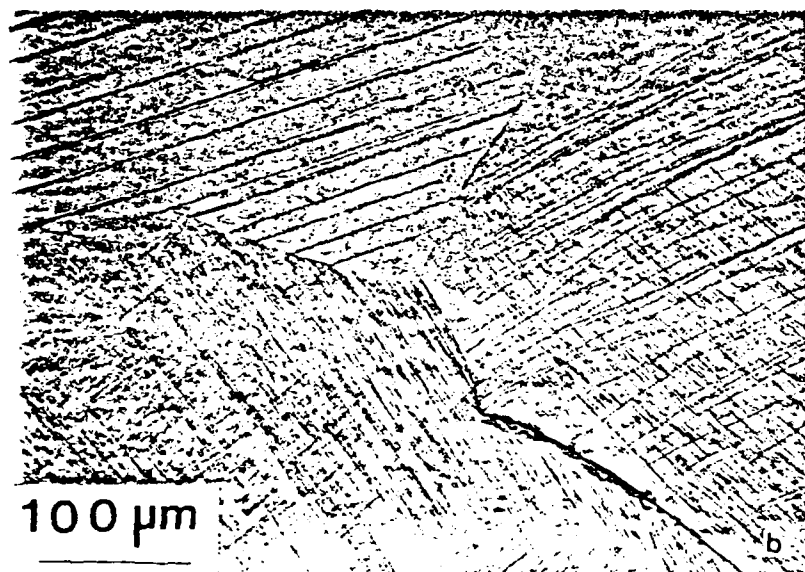
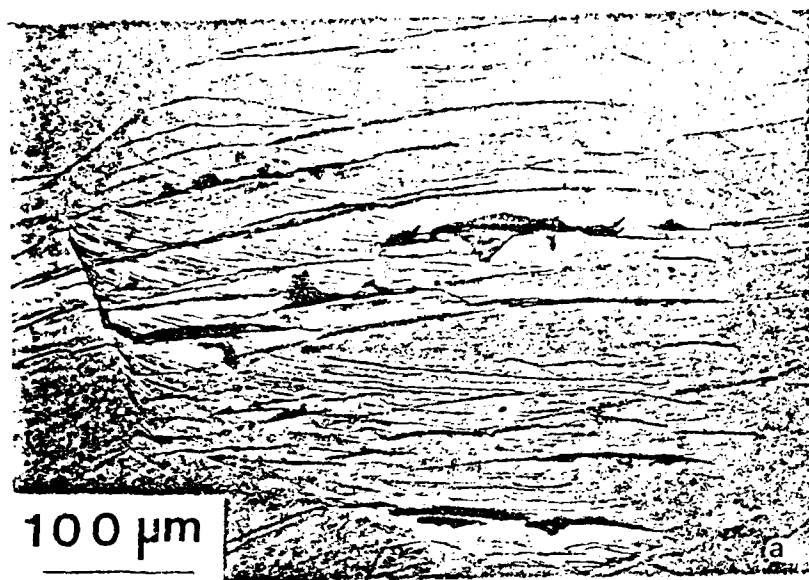


Fig. 6. Replica micrographs showing fatigue crack initiation in the non-implanted specimen (a), and Al implanted specimen (b), at 150 cycles and $\frac{\Delta\epsilon_p}{2} = 8 \times 10^{-3}$.

a stress amplitude of 400 MPa, the increase in life for the implanted samples is almost two orders of magnitude. Similar increases in fatigue life with ion implantation have been associated with compressive residual stresses as discussed before for the case of Cu. The residual stresses are significant since the range of stress amplitudes employed for the present study are well below the elastic limit of the material. The lattice parameter of Ti-24V is about 0.322 ± 0.001 nm and the Goldschmidt's radii of Al, Ti and V are .143, .147 and .136 nm, respectively. Misfit strains due to the implantation of aluminum were calculated and found to be + 1.73%. This should result in a compressive residual stress which enhances the fatigue life in stress controlled conditions.

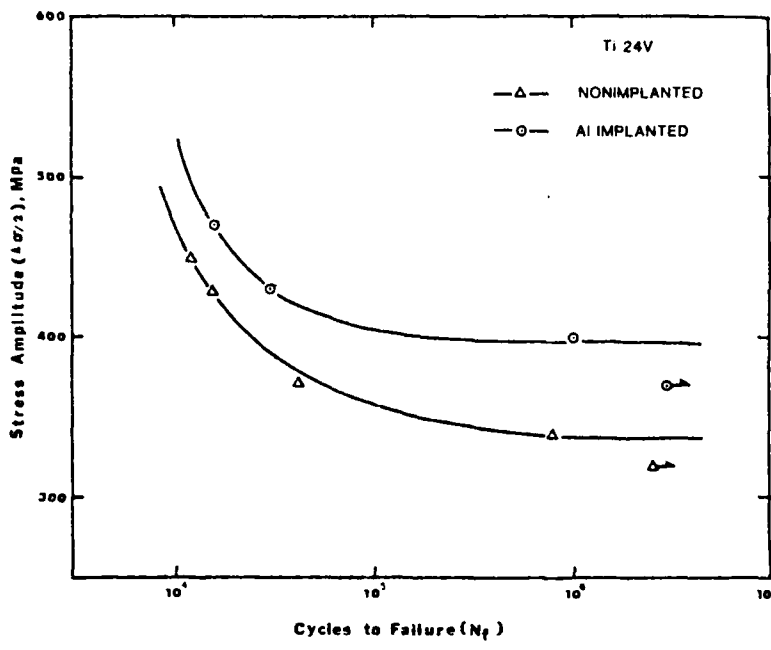


Fig. 7. Stress amplitude vs. Cycles to failure.

In contrast to the above materials, α/β Ti implanted with Al and 4140 steel with N (18) showed a decrease in life time in strain controlled tests. The mechanisms in α/β Ti were discerned by replica study and SEM examination of the surfaces of the samples fatigued to different number of cycles. These studies showed that the decrease in life time was due to an increased number of microcracks in the implanted case as

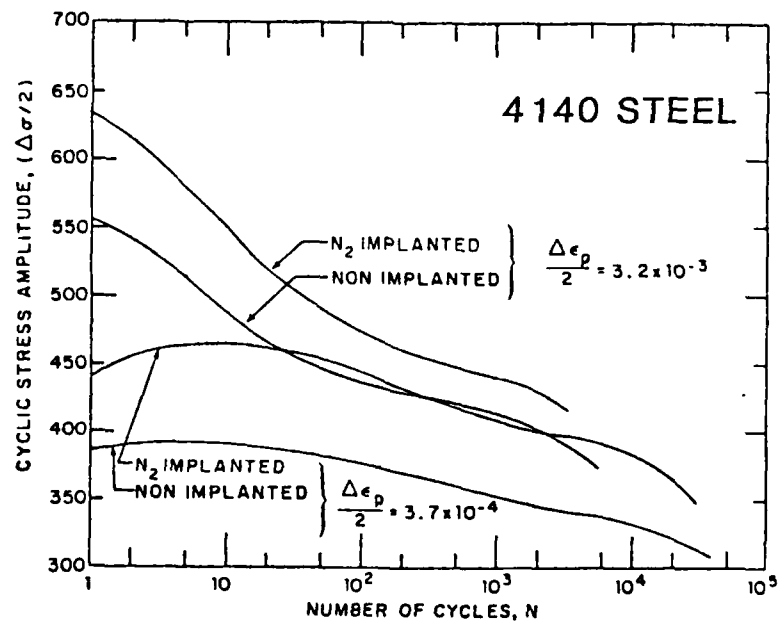


Fig. 8. Cyclic stress amplitude curves for 4140 steel showing the increase in the stress amplitude with N implantation.

observed in the replicas and a transition from wavy to planar slip as observed in the SEM. It was observed that the density of crack initiation sites in the implanted condition was almost two times more than that in the non-implanted, thus easing the linkup of microcracks. Since these microcracks are formed in intense planar slip bands, the driving force for the linkup would be much more due to an additional hydrostatic stress component that results in a decreased fatigue life. In the case of 4140 steel the mechanisms involved in the decrease of fatigue life were not studied. A more interesting finding was that the cyclic stress amplitude increased dramatically by 12-15 percent with nitrogen implantation. This is shown in Figure 8 for two different strain amplitudes. The reason for this is the formation of Fe_4N (γ') precipitates Figure 9, which hardens the surface layer considerably. This hardening increases the high cycle fatigue life and endurance limit, as shown in Figure 10.

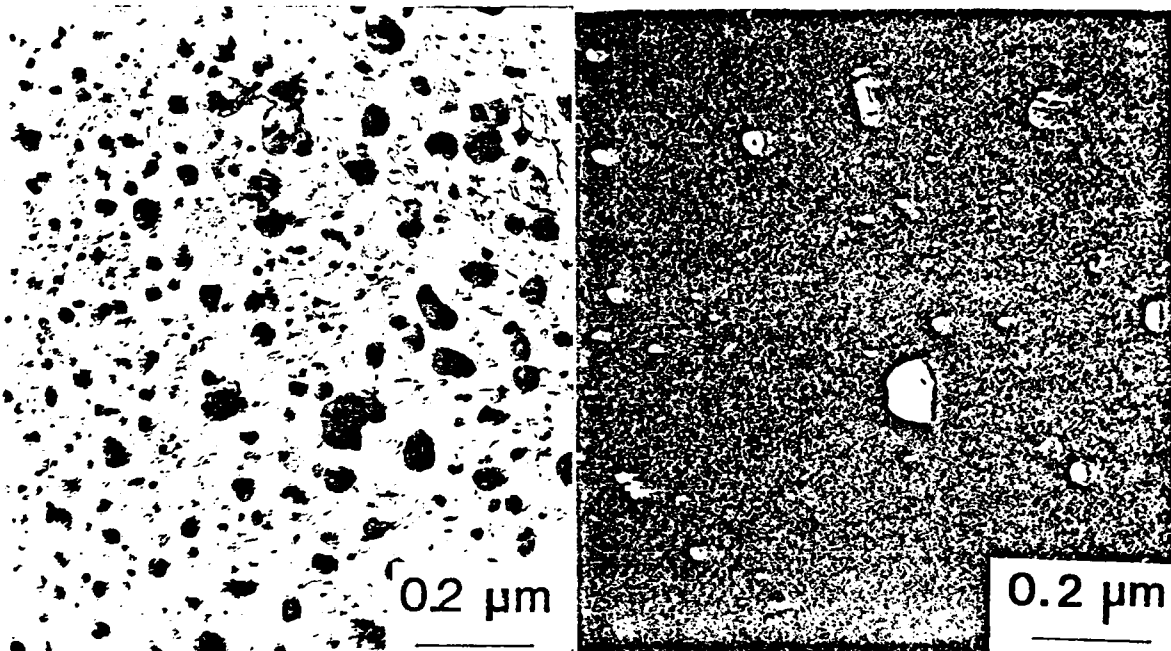


Fig. 9. A pair of bright and dark field TEM's showing the Fe_4N precipitates.

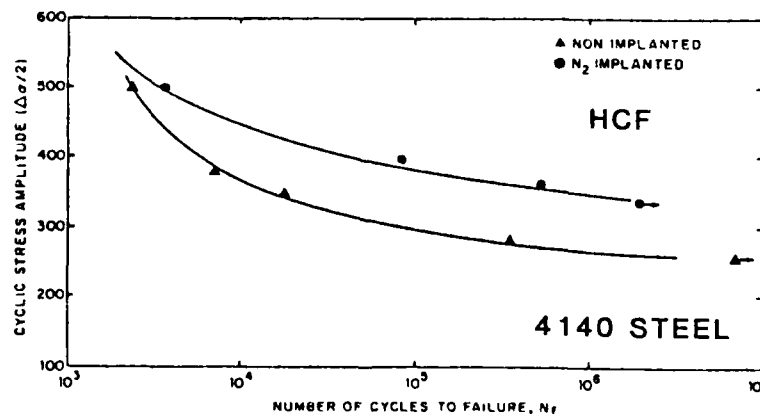


Fig. 10. High-cycle fatigue curve for the 4140 steel showing increased fatigue resistance with implantation.

2. D. High Temperature Studies of Commercial Al Alloy 2124

In a recent investigation (19) we have examined the strain response at high temperatures, under a constant load in a 2124 Al alloy in the unimplanted, as implanted with Fe and Ce and implanted plus annealed conditions. The 2124 alloy was chosen in the peakaged condition and as shown in Figure 11(a), the microstructure consists of $S(Al_2CuMg)$ precipitates within the grains and some grain boundary equilibrium precipitates with the same composition and large Mn dispersoids. Fe and Ce were implanted at 150 keV to achieve a similar penetration depth which was $0.1 \mu m$ and the resulting atomic percent concentrations were 8Fe and 4Ce.

Some implanted TEM foils were mounted in the hot stage of the electron microscope and were observed for microstructural evolution at 473 K. In the as-implanted condition, dislocation loops arising from the collapse of point defect clustering was observed. There was some evidence of microcrystallinity as inferred from the rings of the diffraction pattern. With annealing, much of the damage was removed and precipitation started to occur after 90 minutes of exposure at this temperature. Although the initial precipitates were round and 55 nm in diameter, subsequent annealing resulted in an additional rod shaped precipitates which were 66 nm long. Both these precipitates did not coarsen and the fine dispersion was retained at least for four hours of constant examination. Both Al_3Fe and $Al_{10}Fe_2Ce$ precipitates were observed and these are shown in the micrograph of Figure 11(b).

The retainment of the strength at elevated temperatures in aluminum alloys essentially lies in its ability to maintain thermally stable microstructure. In this context the implant species used in the present work provide excellent candidates due to their extremely small diffusion coefficients. In the preliminary experiments of creep, tests have been conducted in air to observe if any significant changes in creep strain would occur considering that the volume percent of the implanted material is only one hundredth of the total volume of the sample. In these tests a single sample was first loaded to a stress level of 138 Mpa and the temperature was rapidly increased to the desired starting temperature of 505 K by an induction heater. The sample was allowed to creep for a period of three and one half hours and the strain was monitored with a high temperature extensometer. At the end of this period the same sample was used for the next testing temperature of 533 K. This temperature was obtained within a period of two to three minutes and the strain was again monitored for one and one-half hours. In a similar fashion the next test was performed at 573 K. The as-implanted sample failed at the beginning of the third segment of the test and the unimplanted sample failed rapidly at the end of the third segment of the test indicating that the sustenance to creep in the annealed condition was far superior than the other two tested conditions. It was also evident from these tests that the creep strain rates in the as-implanted condition were higher than the rates in the other conditions. The response of creep strain in the first period of testing is shown in Figure 12. The analysis of the data of minimum creep strain rates at the end of each testing period shows that the rates diverge as the test temperature is increased. The present observations are similar to the results obtained by Hall on Mo implanted with heavy ions of Te, In and Ge.

The severe degradation in the creep resistance and early failure of the as-implanted specimen suggests that some drastic alteration in the microstructure has occurred upon ion implantation with Fe and Ce. Considering firstly, that the heavy Fe and Ce ions were used at 150 keV energy, which would produce a large flux of vacancies, and secondly that the grain size of the alloy in the long and long-transverse direction is greater $100 \mu m$, leads us to believe that the vacancies have migrated large distances beneath the surface and coalesced as voids at the grain boundaries. If this possibility exists, then further application of stress at high temperatures might have caused grain boundary failure either by boundary migration or void coalescence. This reasoning would also imply that the void growth and coalescence or boundary migration which led to premature failure took place at a much faster rate than the precipitate nucleation and growth during creep testing under the application of stress.

In the specimens which were annealed at 463K for 10 hours prior to creep testing exhibited stable Al_3Fe and $Al_{10}Fe_2Ce$ microstructure. These would impart both particle and subgrain boundary strengthening to the alloy by blocking dislocation movement, and pinning the subgrains. Whether the annealing treatment eliminated the voids - which could have been formed as discussed above - is difficult to predict. The great improvement in the creep resistance and high failure strains, upon implantation plus annealing

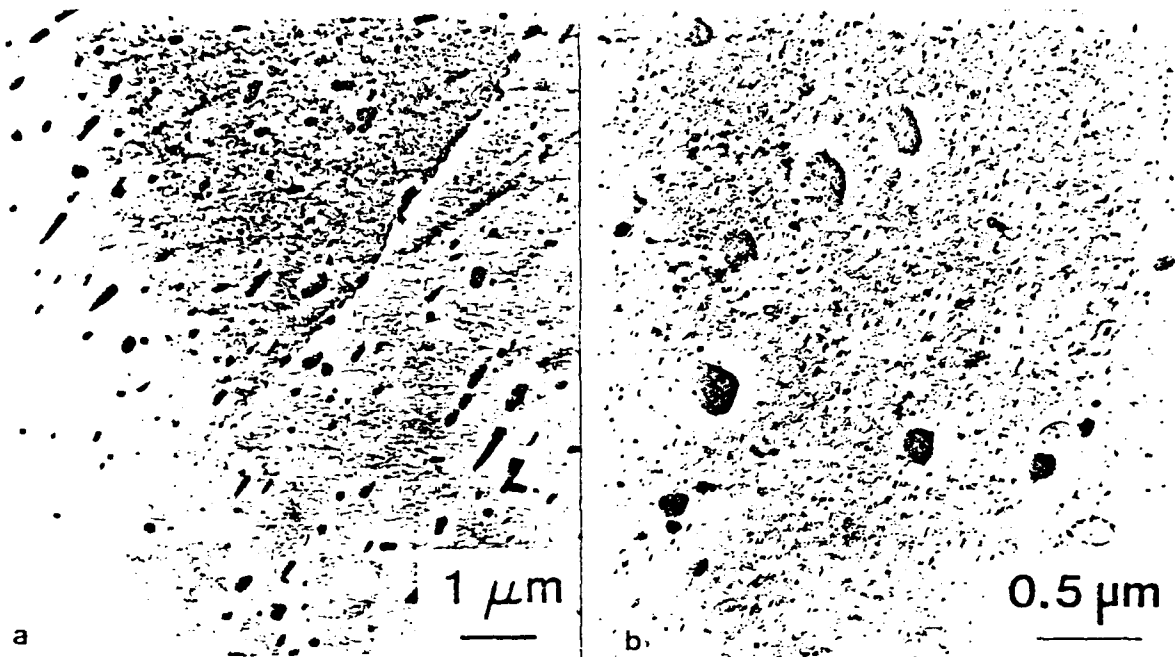


Fig. 11(a). Microstructure of the 2124 Al alloy. (b) Al_3Fe and $Al_{10}Fe_2Ce$ precipitation in the implanted plus annealed alloy.

certainly suggests that the attained precipitate structure plays a major role. Further investigations are currently being conducted to confirm and understand the above proposed mechanisms.

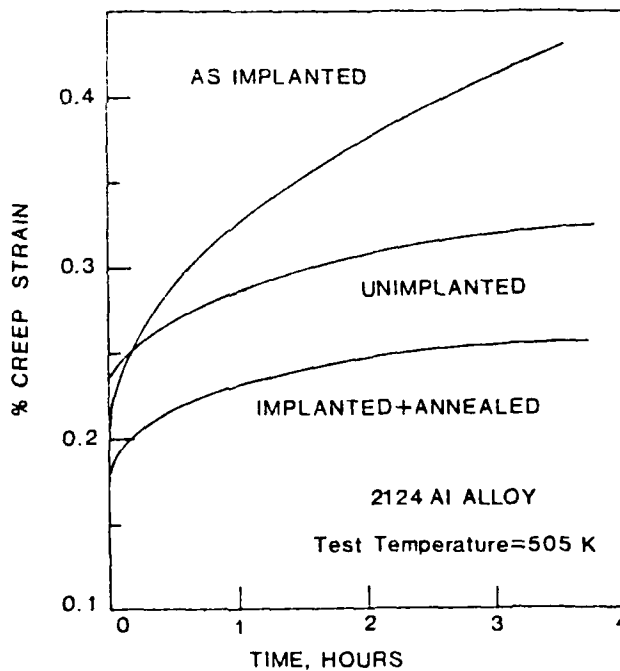


Fig. 12. Creep strain versus time in the 2124 alloy at 138 MPa and $T=505K$.

3. Conclusions

Ion implantation can have a major effect on the cyclic deformation and fatigue life. When the deformation changes to a more homogeneous nature, reversibility of slip could increase which enhances low cycle fatigue life. It is also found that in such a situation the resulting cyclic flow stresses are lower in the implanted as compared to non-implanted. In complex alloys such as steel, nitrogen implantation hardens the surface considerably through dislocation-particle interactions which does not increase the low cycle fatigue life. In high cycle fatigue, compressive residual stresses are beneficial. Tensile residual stresses decrease fatigue life. In steel high cycle fatigue life improves due to a hardened surface layer by dislocation-particle interactions. Generally, ion implantation produces a supersaturated solid solution unless precipitation took place by radiation enhanced diffusion. However precipitation could be controlled by proper thermal annealing treatments after implantation has been performed. This could be exploited to obtain desirable fatigue and high temperature deformation properties, particularly in Al alloys.

4. Acknowledgements

We would like to thank our colleagues who contributed to this work: Dr. S. B. Chakraborty, Dr. K. O. Legg, J. Han and D. Janoff. This research was sponsored by the Office of Naval Research under contract No. 0014-78-C-0270, Dr. Phillip A. Clarkin, Program Manager.

5. References

1. J. K. Hirvonen, ed. *Treatise in Materials Science and Technology - Ion Implantation*, Academic Press, Vol. 13, (1980).
2. V. Ashworth, W. A. Grant and R. P. M. Procter, Eds. *Ion Implantation into Metals*, Pergamon Press, (1982).
3. G. K. Hubler, O. W. Holland, C. R. Clayton and C. W. White, eds. "Ion Implantation and Ion Beam Processing of Materials," Elsevier Science Publishing Co., Inc., (1984).
4. A. Kujore, S. B. Chakraborty, E. A. Starke and K. O. Legg, "The Effect of Ion Implantation on the Fatigue Properties of Polycrystalline Copper," *Nuc. Inst. Meth.* 182/183 (1981), pp. 949-958.
5. I. W. Hall, "The Effect of Ion Implantation on the High Temperature Deformation of Molybdenum," *Met. Trans.* 12A (1981), pp. 2093-2099.
6. M. L. Eben and W. A. Backofen, "Fatigue in Single Crystals of Copper," *Trans. AIME* 215, (1959), pp. 510-520.
7. W. H. Kim and C. Laird, "Crack Nucleation and Stage 1 Propagation in High Strain Fatigue-I. Microscopic and Interferometric Observations," *Acta. Met.*, 26 (1978), pp. 777-787.
8. W. H. Kim and C. Laird, "Crack Nucleation and Stage 1 Propagation in High Strain Fatigue-II Mechanism," *Acta. Met.*, 26, (1978), pp. 789-799.
9. E. Y. Chen and E. A. Starke, Jr., "The Effect of Ion Planting on the Low Cycle Fatigue Behavior of Copper Single Crystals," *Mat. Sci. Eng.* 24 (1976), pp. 209-221.
10. S. B. Chakraborty, A. Kujore and E. A. Starke, Jr., "The Effects of Ion Implantation on Cyclic Stress-Strain Response of Polycrystalline Copper," *Thin Solid Films*, 73, (1980), pp. 209-219.
11. S. B. Chakraborty, S. Spooner and E. A. Starke, Jr., "The Effect of Ion Planting and Ion Implantation on Cyclic Response and Fatigue Crack Initiation in Metals and Alloys," Technical Report 79-2, Office of Naval Research, April 1980.
12. J. M. Poate and A. G. Cullis, "Implantation Metallurgy - Metastable Alloy Formalism" in cf 1., pp. 85-131.

13. S. P. Singhal, H. Herman and J. K. Hirvonen. "Spinodal Decomposition in Amorphous Au - Implanted t." Appl. Phys. Lett. 32, 1 (1978), pp. 25-26.
14. P. Sigmund. "Energy Density and Time Constant of Heavy Ion-Induced Elastic-Collision Spikes in Solids." Appl. Phys. Lett. 25, 3. (1974), pp. 169-171.
15. S. M. Myers. "Implantation Metallurgy - Equilibrium Alloys." in cf. 1, pp. 51-82.
16. K. V. Jata, D. Janoff and E. A. Starke, Jr., "Modulated Structures in Ion Implanted Al-Fe System." in cf. 3 pp. 157-162.
17. K. V. Jata, J. Han, E. A. Starke, Jr., and K. O. Legg. "Ion Implantation Effect on Fatigue Crack Initiation in Ti-24V." Scr. Met. 17, (1983), pp. 479-483.
18. K. V. Jata and E. A. Starke, Jr., "Surface Modification by Ion Implantation - Effects on Fatigue." J. of Metals, 35, 8 (1983), pp. 23-27.
19. K. V. Jata and G. K. Hubler. "The Effect of Fe and Ce Ion Implantation on the High Temperature Deformation Behavior of a 2124 Al Alloy." Accepted for Publication in J. of Vac. Sci. and Tech.

DISTRIBUTION LIST

Copy No.

- 1 (N00014)
Office of Naval Research
800 N. Quincy Street
Arlington, VA 22217-5000
Attention: Leader, Materials Division
Associate Director for Engineering Sciences
- 2 Office of Naval Research Resident
Representative, N66002
Joseph Henry Building, Room 623
2100 Pennsylvania Avenue, N.W.
Washington, DC 20037
Attention: Mr. Michael McCracken
Administrative Contracting Officer
- 3 - 8 Director, N00173
Naval Research Laboratory
Washington, DC 20375
Attention: Code 2627
- 9 - 20 Defense Technical Information Center, S47031
Bldg. 5, Cameron Station
Alexandria, VA 22314
- 21 - 23 E. A. Starke, Jr.
Dean
- 24 - 25 K. V. Jata, Materials Science
- 26 K. R. Lawless, Materials Science
- 27 - 28 E. H. Pancake
Clark Hall
- 29 SEAS Publications Files

JO#6748:pms

UNIVERSITY OF VIRGINIA
School of Engineering and Applied Science

The University of Virginia's School of Engineering and Applied Science has an undergraduate enrollment of approximately 1,500 students with a graduate enrollment of approximately 500. There are 125 faculty members, a majority of whom conduct research in addition to teaching.

Research is a vital part of the educational program and interests parallel academic specialties. These range from the classical engineering disciplines of Chemical, Civil, Electrical, and Mechanical and Aerospace to newer, more specialized fields of Biomedical Engineering, Systems Engineering, Materials Science, Nuclear Engineering and Engineering Physics, Applied Mathematics and Computer Science. Within these disciplines there are well equipped laboratories for conducting highly specialized research. All departments offer the doctorate; Biomedical and Materials Science grant only graduate degrees. In addition, courses in the humanities are offered within the School.

The University of Virginia (which includes approximately 1,500 full-time faculty and a total full-time student enrollment of about 16,000), also offers professional degrees under the schools of Architecture, Law, Medicine, Nursing, Commerce, Business Administration, and Education. In addition, the College of Arts and Sciences houses departments of Mathematics, Physics, Chemistry and others relevant to the engineering research program. The School of Engineering and Applied Science is an integral part of this University community which provides opportunities for interdisciplinary work in pursuit of the basic goals of education, research, and public service.